


Fast elementwise operations on tensor trains with alternating cross interpolation

Marc K. Ritter 

Center for Computational Quantum Physics, Flatiron Institute, 162 5th Avenue, New York, NY 10010, USA

(Dated: April 2, 2026)

Tensor trains (TTs), also known as matrix product states (MPS), are compressed representations of high-dimensional data that can be efficiently manipulated to perform calculations on the data. In many applications, such as TT-based solvers for nonlinear partial differential equations, the most expensive step is an elementwise multiplication or similar elementwise operation on multiple TTs. Known error-controlled algorithms for such operations scale as $\mathcal{O}(\chi^4)$, where χ is the TT rank. If the rank of the output is smaller than χ^2 , it is possible to formulate algorithms with better scaling. In this work, we present the alternating cross interpolation (ACI) algorithm that performs such operations in $\mathcal{O}(\chi^3)$, while maintaining error control. We demonstrate these properties on benchmark problems, achieving a significant speedup for TT ranks that are commonly encountered in practical applications.

INTRODUCTION

High-dimensional problems and problems involving a large range of length scales are common challenges in computational physics, as naïve approaches to such problems quickly exhaust the available computational resources. A paradigmatic example is finding the ground state of an interacting many-body quantum system, of a high-dimensional problem, is commonly done using a compressed tensor network representation of the solution [1, 2]. The most well-known of these methods is the density-matrix renormalization group (DMRG), which relies on tensor trains (TTs), also known as matrix product states (MPSs) [3–5]. TT approaches have been used for many other high-dimensional problems, such as evaluation of Feynman diagrams [6], representing orbitals in quantum chemistry [7], and options pricing in financial mathematics [8–11]. Similarly, TTs can be used to solve problems of many length scales in a compressed format, such as evaluating Bethe–Salpeter equations [12, 13], integrating over Brillouin zones [14], calculating strain in 2D super-moiré materials [15], and simulating fluid dynamics [16–20].

In many of these applications, the limiting factor is the $\mathcal{O}(\chi^4)$ runtime scaling of known algorithms for multiplication and contraction of TTs [21–24], where χ is the rank of the input TT. Multiplication of TTs is typically performed by contracting the TT with Kronecker- δ tensor cores [12, 13, 25]. In the general case, where $\chi' = \chi^2$, it is not possible to decrease the scaling below $\mathcal{O}(\chi^4)$, since the resulting TT has $\mathcal{O}(\chi'^2) = \mathcal{O}(\chi^4)$ elements. In practical applications, such as differential equation solvers, the case $\chi' \in \mathcal{O}(\chi)$ is, however, very common. For example, the input TT might correspond to the solution at a particular time step, and the result is the solution at the next time step. In this case, χ is related to the correlations between different variables and length scales, which are governed by the differential equation to be solved. Therefore, they do not tend to increase infinitely at exponential speed. For

$\chi' \in \mathcal{O}(\chi)$, it is possible to formulate algorithms that scale as $\mathcal{O}(\chi^3)$. Such algorithms are particularly relevant for TT-based solvers for nonlinear differential equations, such as the Gross–Pitaevskii equation or the Navier–Stokes equations, as the cost of evaluating them is usually entirely dominated by the cost of evaluating elementwise products in the nonlinear terms [16–20, 25, 26].

This work presents an algorithm, called alternating cross interpolation (ACI), which computes elementwise operations, such as the Hadamard product, in an error-controlled way. It is closely related to the 2-site tensor cross interpolation (TCI) algorithm [6, 27–32], combined with ideas from the alternating minimal energy method (AMEn) [33]. It is also inspired by the recursive sketched interpolation (RSI) algorithm presented in Ref. 34, which scales as our ACI algorithm, but does not offer the same error control. To the best of our knowledge, other algorithms for efficient evaluation of elementwise operations that have been proposed in prior work [35–37] do not achieve scaling below $\mathcal{O}(\chi^4)$ without imposing further assumptions.

ALTERNATING CROSS INTERPOLATION ALGORITHM

Problem statement. Given a function $f : \mathbb{C}^N \rightarrow \mathbb{C}$, and N tensor trains

$$x_{\sigma_1, \dots, \sigma_{\mathcal{L}}}^n := \begin{array}{ccccccc} X_1^n & X_2^n & \dots & X_{\mathcal{L}}^n \\ * \square & \square & \dots & \square * \\ \sigma_1 & \sigma_2 & \dots & \sigma_{\mathcal{L}} \end{array}, \quad n = 1, \dots, N, \quad (1)$$

each with indices $(\sigma_1, \dots, \sigma_{\mathcal{L}}) =: \boldsymbol{\sigma} \in \mathbb{S} = \mathbb{S}_1 \otimes \dots \otimes \mathbb{S}_{\mathcal{L}}$, we would like to obtain a tensor train Y that approximates

$$y_{\boldsymbol{\sigma}} := \begin{array}{ccccccc} Y_1 & Y_2 & \dots & Y_{\mathcal{L}} \\ * \square & \square & \dots & \square * \\ \sigma_1 & \sigma_2 & \dots & \sigma_{\mathcal{L}} \end{array} \approx f(x_{\boldsymbol{\sigma}}^1, \dots, x_{\boldsymbol{\sigma}}^N) \quad (2)$$

for all values of σ . In practice, this means Y should fulfill

$$\|y - f(x^1, \dots, x^N)\|_\infty = \max_{\sigma \in \mathbb{S}} |y_\sigma - f(x_\sigma^1, \dots, x_\sigma^N)| \leq \tau \quad (3)$$

for some user-specified tolerance τ . Note that f operates *elementwise*: at each point σ , the output of f depends only on the value of $x_\sigma^1, \dots, x_\sigma^N$, all evaluated at the same point σ . Common elementwise operations include addition of TTs and the Hadamard product $x^1 \odot \dots \odot x^N$.

Overview. ACI is an alternating optimization algorithm that sweeps across the tensor train, performing local updates at each pair of sites $\ell, \ell + 1$. Efficient evaluation of the local updates is achieved by combining the CI-canonical gauge for the solution y with frame matrices for the inputs x . Each of these steps is explained below using tensor network diagrams [2]; a pseudocode in algebraic notation can be found in Sec. S-2 of the supplemental material [38].

Alternating optimization. Alternating optimization is a strategy to approach large optimization problems on TTs by casting the global optimization problem into a series of small local problems. The idea is that successively solving each local problem eventually leads to global convergence. The most famous example of such a method is the density matrix renormalization group (DMRG), which finds the ground state of a quantum system by solving a series of local eigenvalue problems [2, 4, 5].

The global problem considered in this work is to find tensors $Y_1, \dots, Y_{\mathcal{L}}$ that satisfy Eq. (3), ideally with quasi-optimal bond dimensions χ'_1, \dots, χ'_N . We approach this problem using 2-site alternating optimization, where we iterate over pairs of neighbouring sites. In each iteration, the algorithm solves the local problem of finding the optimal tensors Y_ℓ and $Y_{\ell+1}$, given current values of all other tensors $Y_{\ell' \notin \{\ell, \ell+1\}}$. The solution y is then updated with the new Y_ℓ and $Y_{\ell+1}$ (*local update*), before moving on to the next local problem.

The remainder of this section explains how to formulate a cheaply solvable local problem that leads to a solution of Eq. (3). To this end, we fix the gauge freedom in y to the CI-canonical gauge.

CI-canonical gauge. The CI-canonical gauge is defined through ordered index sets \mathcal{I}_ℓ and \mathcal{J}_ℓ [32]. The left index sets $\mathcal{I}_\ell \subseteq \mathbb{S}_1 \otimes \dots \otimes \mathbb{S}_\ell$ contain multi-indices $i = (i_1, \dots, i_\ell)$ that can be used as indices to Y_1, \dots, Y_ℓ . Analogously, the right index sets $\mathcal{J}_\ell \subseteq \mathbb{S}_\ell \otimes \dots \otimes \mathbb{S}_{\mathcal{L}}$ contain multi-indices $j = (j_\ell, \dots, j_{\mathcal{L}})$ on $Y_\ell, \dots, Y_{\mathcal{L}}$. Concatenating a multi-index $i = (i_1, \dots, i_\ell) \in \mathcal{I}_\ell$ with a multi-index $j = (j_{\ell+1}, \dots, j_{\mathcal{L}}) \in \mathcal{J}_{\ell+1}$ to $ij = (i_1, \dots, i_\ell, j_{\ell+1}, \dots, j_{\mathcal{L}})$ results in an index into the full tensor train y .

We can now define *slices* P_ℓ, T_ℓ and Π_ℓ of the tensor train y as

$$i \text{---} \diamond \text{---} j := y_{ij}, \quad i \in \mathcal{I}_\ell, \quad j \in \mathcal{J}_{\ell+1}; \quad (4a)$$

$$i \text{---} \square \text{---} j := y_{i\sigma_\ell j}, \quad i \in \mathcal{I}_{\ell-1}, \quad j \in \mathcal{J}_{\ell+1}; \quad (4b)$$

$$i \text{---} \square \text{---} j := y_{i\sigma_\ell \sigma_{\ell+1} j}, \quad i \in \mathcal{I}_{\ell-1}, \quad j \in \mathcal{J}_{\ell+2}. \quad (4c)$$

In CI-canonical gauge, y is given by [32]

$$y_{\sigma_1, \dots, \sigma_N} = \begin{array}{c} T_1 \quad P_1^{-1} \quad T_2 \quad P_2^{-1} \quad \dots \quad T_{\mathcal{L}} \\ \square \text{---} \square \text{---} \square \text{---} \square \text{---} \square \text{---} \square \text{---} \square \\ \sigma_1 \quad \sigma_2 \quad \dots \quad \sigma_{\mathcal{L}} \end{array} \quad (5)$$

The tensors Y_ℓ in Eq. (2) can be recovered by multiplying all P_ℓ^{-1} to the left or the right, e.g. $Y_\ell = T_\ell P_\ell^{-1}$.

Local problem. We are now ready to formulate a local problem corresponding to Eq. (3). We assume for the moment that good index sets $\mathcal{I}_\ell, \mathcal{J}_\ell$ for y are known. Optimization of the index sets is discussed in a separate section below. Given these index sets, each local tensor in y can be computed directly as

$$P_\ell \text{---} \diamond \text{---} j = f(x_{i_j}^1, \dots, x_{i_j}^N); \quad i \text{---} \square \text{---} j = f(x_{i\sigma_\ell j}^1, \dots, x_{i\sigma_\ell j}^N). \quad (6)$$

Thus, the local problem is reduced to computing the slices $x_{i_j}^n$ and $x_{i\sigma_\ell j}^n$ on the index sets required for y . Evaluating a TT at a particular choice of indices costs $\mathcal{O}(\chi^3 \mathcal{L})$. Evaluating Eqs. (6) naïvely at each combination of i, σ_ℓ , and j would therefore scale as $\mathcal{O}(d\chi^3 \chi' \mathcal{L} N)$. This cost can be reduced by precomputing left and right *frame matrices* [33],

$$L_\ell^n \text{---} \beta \equiv \begin{array}{c} X_1^n \quad X_2^n \quad \dots \quad X_\ell^n \\ \square \text{---} \square \text{---} \dots \text{---} \square \text{---} \beta \\ i \quad i_1 \quad i_2 \quad \dots \quad i_\ell \end{array}, \quad \alpha \text{---} \square \equiv \begin{array}{c} X_\ell^n \quad X_{\ell+1}^n \quad \dots \quad X_{\mathcal{L}}^n \\ \alpha \text{---} \square \text{---} \square \text{---} \dots \text{---} \square \text{---} \alpha \\ j \quad j_\ell \quad j_{\ell+1} \quad \dots \quad j_{\mathcal{L}} \end{array}, \quad (7)$$

with $i = (i_1, \dots, i_\ell) \in \mathcal{I}_\ell$ and $j = (j_\ell, \dots, j_{\mathcal{L}}) \in \mathcal{J}_\ell$. There is an efficient method to compute L_ℓ^n and R_ℓ^n provided the index sets \mathcal{I}_ℓ and \mathcal{J}_ℓ satisfy the *nesting conditions* [6, 32]: The set $\mathcal{I}_{\ell+1}$ is nested with respect to \mathcal{I}_ℓ (denoted $\mathcal{I}_\ell < \mathcal{I}_{\ell+1}$) if $\forall (i_1, \dots, i_\ell, i_{\ell+1}) \in \mathcal{I}_{\ell+1}$, removing the last index, $i_{\ell+1}$, results in an element of \mathcal{I}_ℓ : $(i_1, \dots, i_\ell) \in \mathcal{I}_\ell$. Analogously, $\mathcal{J}_{\ell-1} > \mathcal{J}_\ell$ if $\forall (j_{\ell-1}, j_\ell, \dots, j_{\mathcal{L}}) \in \mathcal{J}_{\ell-1}$: $(j_\ell, \dots, j_{\mathcal{L}}) \in \mathcal{J}_\ell$. If $\mathcal{I}_\ell < \mathcal{I}_{\ell+1}$, $L_{\ell+1}^n$ can be obtained from L_ℓ^n by contracting

$$L_{\ell+1}^n \text{---} \beta = \begin{array}{c} L_\ell^n \quad X_{\ell+1}^n \\ \square \text{---} \square \text{---} \square \text{---} \beta \\ i \quad (i_1, \dots, i_\ell) i_{\ell+1} \end{array} \quad (8a)$$

and truncating the index i such that $i \in \mathcal{I}_{\ell+1}$. Analogously, $R_{\ell-1}^n$ is obtained efficiently by contracting

$$\alpha \text{---} \square = \begin{array}{c} R_{\ell-1}^n \quad X_{\ell-1}^n \quad R_\ell^n \\ \alpha \text{---} \square \text{---} \square \text{---} \square \\ j \quad j_{\ell-1} (j_\ell, \dots, j_{\mathcal{L}}) \end{array} \quad (8b)$$

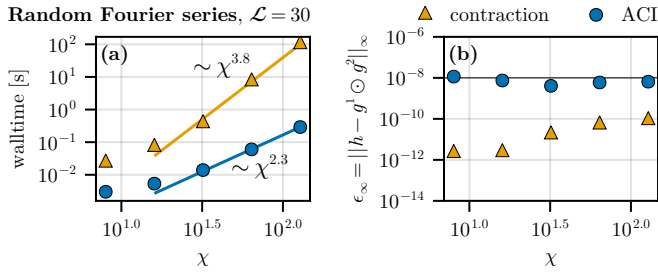


FIG. 2. Hadamard product of random Fourier series, Eq. (16). Two functions of the form (15) are represented as TT with $\mathcal{L} = 30$ quantics indices, then multiplied elementwise with a tolerance of $\tau = 10^{-8}$ using the ACI algorithm (this work, blue circles), and an algorithm based on MPO-MPS contraction (yellow triangles). (a) Runtime needed to perform the multiplication. Lines are fitted power laws $\sim \chi^p$, which are consistent with the theoretical scaling of $\mathcal{O}(\chi^3)$ for ACI and $\mathcal{O}(\chi^4)$ for the contraction-based Hadamard product. Runtimes were measured using a single thread on an AMD EPYC 9474F processor. (b) Maximum error between the ACI output h and the exact product $f \odot g$. Both methods consistently reach the error tolerance $\tau = 10^{-8}$ (black line).

the quantics representation [42]

$$\frac{x - x_{\min}}{x_{\max} - x_{\min}} = \sum_{\ell=1}^{\mathcal{L}} 2^{-\ell} \sigma_\ell \quad (13)$$

with $\mathcal{L} = 25$ binary indices σ_ℓ . Quantics tensor trains (QTT) representing g_\pm are then obtained using 2-site TCI [32], and used as input to ACI.

As shown in Fig. 1(a), the peaks of f_\pm move apart with increasing δ , whereas $h = g_+ \odot g_-$ always has a peak around $x = 0$. For large δ , the optimal index sets for h are therefore very different from those for g_\pm [34]. This simple example thus verifies that ACI is capable of discovering structure in the solution which is not present in the inputs: Fig. 1 shows that the maximum error between the ACI output and the exact solution,

$$\epsilon_\infty = \|h - g_+ \odot g_-\|_\infty = \max_x |h(x) - g_+(x)g_-(x)|, \quad (14)$$

decreases exponentially with increasing bond dimension χ' , down to numerical accuracy $\epsilon_{\text{Float64}} \approx 10^{-14}$. As the discretization grid contains too many points for explicit evaluation of ϵ_∞ , the error is approximated as the maximum over 10^3 random samples in this and the following examples.

Random Fourier series. To benchmark the runtime scaling and accuracy of the algorithm across many bond dimensions, we generate two random Fourier series

$$g^n(x) = \sum_{k=0}^K \hat{g}_k^n e^{ikx}; \quad n = 1, 2 \quad (15)$$

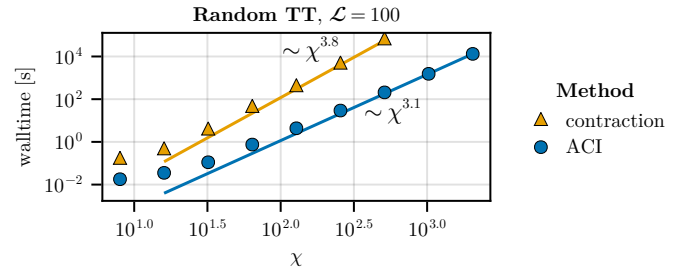


FIG. 3. Similar to Fig. 2(a), but now for the Hadamard product of random TT. Instead of setting a fixed tolerance, the output bond dimension was set to $\chi' = \chi$ here.

with $K+1$ complex Fourier coefficients \hat{g}_k^n , whose real and imaginary parts are independently drawn from a uniform distribution on $[0, 1]$. The coefficients are then normalized such that $\sum_k |\hat{g}_k^n|^2 = 1$. We discretize these functions on the interval $x \in [0, 1)$ using the quantics representation (Eq. (13)) and obtain a QTT using 2-site TCI [32]. Since the Fourier spectrum of f and g is band-limited with maximum frequency K , the QTT have bond dimension $\chi \in \mathcal{O}(\sqrt{K})$ [43]. Multiplying them generates a new function,

$$\begin{aligned} h(x) &= g^1(x)g^2(x) = \sum_{k=0}^K \sum_{k'=0}^K \hat{g}_k^1 \hat{g}_{k'}^2 e^{i(k+k')x} = \\ &= \sum_{q=0}^{2K} \left[\sum_{q'=-q}^q \hat{g}_{(q+q')/2}^1 \hat{g}_{(q-q')/2}^2 \right] e^{iqx} = \sum_{q=0}^{2K} \hat{h}_q e^{iqx}, \end{aligned} \quad (16)$$

with up to $2K+1$ coefficients \hat{h}_q , which again has a bond dimension $\chi' \in \mathcal{O}(\sqrt{K})$.

The runtime needed for the elementwise multiplication is shown in Fig. 2(a). Using ACI, it scales $\sim \chi^{2.3}$, which is consistent with the theoretical asymptotic scaling of $\mathcal{O}(\chi^3)$, accounting for the fact that χ may not be large enough to reach the asymptotic regime. For comparison, we compute the Hadamard product based on contracting with a Kronecker- δ kernel. We observe a scaling of runtime $\sim \chi^{3.8}$, consistent with the theoretical scaling of $\mathcal{O}(\chi^4)$. Already at moderate bond dimensions of $\chi \approx 100$, ACI achieves a speedup of a factor 10^2 over the contraction algorithm. As shown in Fig. 2(b), both methods reach the requested precision of $\tau = 10^{-8}$ at all data points.

Random TT. To investigate the runtime scaling for larger χ , we multiply input TT that have been generated with random components drawn from a uniform distribution. Except for normalization, this is equivalent to multiplying random wave functions. The exact result of this multiplication has bond dimension $\chi' = \chi^2$, but we apply the algorithms in a mode where we limit χ' to $\chi' \leq \chi$, instead opting to increase the truncation error. The resulting runtimes are shown in Fig. 3, and demon-

strate scaling consistent with the theoretical $\mathcal{O}(\chi^4)$ for the TT contraction algorithm and $\mathcal{O}(\chi^3)$ for ACI.

CONCLUSIONS AND OUTLOOK

We have presented the alternating cross interpolation (ACI) algorithm for computing elementwise operations on tensor trains (TT). In benchmarks focused on computing Hadamard products of TT, we have demonstrated that the runtime scaling of ACI is $\mathcal{O}(\chi^3)$ when the output bond dimension is $\chi' \in \mathcal{O}(\chi)$, while maintaining error control through optimization of index sets. In three examples, we have shown three key properties: ACI converges down to numerical accuracy provided the output bond dimension χ' is large enough; ACI dynamically adjusts χ' according to the specified error tolerance; and when $\chi' \in \mathcal{O}(\chi)$, ACI scales as $\mathcal{O}(\chi^3)$ over many orders of magnitude. The combination of these properties is unique to ACI.

These properties make ACI the method of choice for implementing nonlinearities in nonlinear differential equation solvers using TT. In many nonlinear differential equations, all TT contractions are contractions with TT operators of constant, small bond dimension, such as the Fourier transform [44, 45] or finite-difference derivative operators [16, 46], thus leaving elementwise operations necessary to evaluate nonlinearities as the only step scaling with $\mathcal{O}(\chi^4)$. For instance, TT-based solvers for computational fluid dynamics are limited by the evaluation of the nonlinear convection term [16, 19, 20]. In these settings, switching to ACI with its improved scaling of $\mathcal{O}(\chi^3)$ will result in improving the entire solver's scaling. For further speedup, it is straightforward to use ACI within the patched elementwise multiplication scheme of Ref. [47].

In other settings, such as evaluating equations arising in diagrammatic treatment of many-body theory, the presence of TT contractions scaling as $\mathcal{O}(\chi^4)$ means that applying the ACI algorithm will improve the prefactor, but not the scaling of the total runtime [13]. Nevertheless, improving prefactors is still desirable for practical applications, and using ACI removes the first of two bottlenecks in these applications, such that any improvement to TT contraction algorithms directly leads to speedup of TT-based solvers.

As for the algorithm itself, there are two obvious directions for future work. Firstly, it is straightforward to generalize it to tree-shaped tensor networks in the same manner as TCI [48]. Secondly, the structural similarity of ACI's local updates to RSI's sketching suggests that index sets used in CI-based algorithms can be understood as a particular type of sketch [34]. With sketching ideas being used in different settings to improve performance or reduce the runtime scaling of TT operations, a more complete understanding of the relation between different sketches and how CI fits into that framework may be fruitful.

Code availability. All code and data necessary to reproduce the figures in this paper are available online [49]. An implementation of the ACI algorithm is publicly available [50] as part of the tensor4all open-source libraries [51].

Acknowledgments. The author acknowledges useful discussions with J. von Delft, L. Devos, M. Frankenhach, O. Kovalska, M. Menon, I. V. Oseledets, D. V. Savostyanov, and E. M. Stoudenmire. The author thanks J. von Delft, L. Devos, M. Frankenhach, O. Kovalska, and H. Shinaoka for feedback on the manuscript. The author thanks L. Devos for providing a contraction-based Hadamard product implementation based on MPSKit.jl [40] and TensorKit.jl [41]. The Flatiron Institute is a division of Simons Foundation.

* mritter@flatironinstitute.org

- [1] M. C. Bañuls, Tensor network algorithms: A route map, *Annual Review of Condensed Matter Physics* **14**, 173 (2023).
- [2] R. Orús, A practical introduction to tensor networks: Matrix product states and projected entangled pair states, *Annals of Physics* **349**, 117 (2014).
- [3] S. R. White, Density matrix formulation for quantum renormalization groups, *Physical Review Letters* **69**, 2863 (1992).
- [4] I. P. McCulloch, From density-matrix renormalization group to matrix product states, *Journal of Statistical Mechanics: Theory and Experiment* **2007**, P10014 (2007), [cond-mat/0701428](https://arxiv.org/abs/cond-mat/0701428).
- [5] U. Schollwöck, The density-matrix renormalization group in the age of matrix product states, *Annals of Physics January 2011 Special Issue*, **326**, 96 (2011).
- [6] Y. Núñez Fernández, M. Jeannin, P. T. Dumitrescu, T. Kloss, J. Kaye, O. Parcollet, and X. Waintal, Learning Feynman diagrams with tensor trains, *Physical Review X* **12**, 041018 (2022).
- [7] N. Jolly, Y. N. Fernández, and X. Waintal, *Tensorized orbitals for computational chemistry* (2023), 2308.03508.
- [8] L. Arenstein and M. Kastoryano, *Full grid solution for multi-asset options pricing with tensor networks* (2025), 2601.00009.
- [9] K. Glau, D. Kressner, and F. Statti, Low-rank tensor approximation for chebyshev interpolation in parametric option pricing, *SIAM Journal on Financial Mathematics* **11**, 897 (2020).
- [10] M. Kastoryano and N. Pancotti, *A highly efficient tensor network algorithm for multi-asset fourier options pricing* (2022), 2203.02804.
- [11] R. Sakurai, H. Takahashi, and K. Miyamoto, Learning parameter dependence for fourier-based option pricing with tensor trains, *Mathematics* **13**, 1828 (2025), 2405.00701.
- [12] H. Shinaoka, M. Wallerberger, Y. Murakami, K. Nogaki, R. Sakurai, P. Werner, and A. Kauch, Multiscale space-time ansatz for correlation functions of quantum systems based on quantics tensor trains, *Physical Review X* **13**, 021015 (2023).
- [13] S. Rohshap, M. K. Ritter, H. Shinaoka, J. von Delft,

- M. Wallerberger, and A. Kauch, Two-particle calculations with quantics tensor trains: Solving the parquet equations, *Physical Review Research* **7**, 023087 (2025).
- [14] M. K. Ritter, Y. Núñez Fernández, M. Wallerberger, J. von Delft, H. Shinaoka, and X. Waintal, Quantics tensor cross interpolation for high-resolution parsimonious representations of multivariate functions, *Physical Review Letters* **132**, 056501 (2024).
- [15] A. O. Fumega, M. Niedermeier, and J. L. Lado, Correlated states in super-moiré materials with a kernel polynomial quantics tensor cross interpolation algorithm, *2D Materials* **12**, 015018 (2024).
- [16] N. Gourianov, M. Lubasch, S. Dolgov, Q. Y. van den Berg, H. Babae, P. Givi, M. Kiffner, and D. Jaksch, A quantum-inspired approach to exploit turbulence structures, *Nature Computational Science* **2**, 30 (2022).
- [17] E. Kornev, S. Dolgov, K. Pinto, M. Pfitsch, M. Perelshtein, and A. Melnikov, Numerical solution of the incompressible navier-stokes equations for chemical mixers via quantum-inspired tensor train finite element method (2023), 2305.10784.
- [18] R. D. Peddinti, S. Pisoni, A. Marini, P. Lott, H. Argenterieri, E. Tiunov, and L. Aolita, Quantum-inspired framework for computational fluid dynamics, *Communications Physics* **7**, 1 (2024).
- [19] N. Gourianov, P. Givi, D. Jaksch, and S. B. Pope, Tensor networks enable the calculation of turbulence probability distributions, *Science Advances* **11**, eads5990 (2025).
- [20] L. Hölscher, P. Rao, L. Müller, J. Klepsch, A. Luckow, T. Stollenwerk, and F. K. Wilhelm, Quantum-inspired fluid simulation of two-dimensional turbulence with GPU acceleration, *Physical Review Research* **7**, 013112 (2025).
- [21] E. M. Stoudenmire and S. R. White, Minimally entangled typical thermal state algorithms, *New Journal of Physics* **12**, 055026.
- [22] B.-B. Chen, L. Chen, Z. Chen, W. Li, and A. Weichselbaum, Exponential thermal tensor network approach for quantum lattice models, *Physical Review X* **8**, 031082 (2018).
- [23] L. Ma, M. Fishman, E. M. Stoudenmire, and E. Solomonik, Approximate contraction of arbitrary tensor networks with a flexible and efficient density matrix algorithm, *Quantum* **8**, 1580 (2024).
- [24] C. Camaño, E. N. Epperly, and J. A. Tropp, Successive randomized compression: A randomized algorithm for the compressed MPO-MPS product, *Quantum* **10**, 2022 (2026), 2504.06475.
- [25] A. Bou-Comas, M. Płodzień, L. Tagliacozzo, and J. J. García-Ripoll, Quantics tensor train for solving Gross-Pitaevskii equation (2025), 2507.03134.
- [26] Q.-C. Chen, I.-K. Liu, J.-W. Li, and C.-M. Chung, Solving the Gross-Pitaevskii equation with quantic tensor trains: Ground states and nonlinear dynamics (2025), 2507.04279.
- [27] I. Oseledets and E. Tyrtyshnikov, TT-cross approximation for multidimensional arrays, *Linear Algebra and its Applications* **432**, 70 (2010).
- [28] I. V. Oseledets, Tensor-train decomposition, *SIAM Journal on Scientific Computing* **33**, 2295 (2011).
- [29] D. Savostyanov and I. Oseledets, Fast adaptive interpolation of multi-dimensional arrays in tensor train format, in *The 2011 International Workshop on Multidimensional (nD) Systems* (IEEE, 2011) pp. 1–8.
- [30] D. V. Savostyanov, Quasioptimality of maximum-volume cross interpolation of tensors, *Linear Algebra and its Applications* **458**, 217 (2014).
- [31] S. Dolgov and D. Savostyanov, Parallel cross interpolation for high-precision calculation of high-dimensional integrals, *Computer Physics Communications* **246**, 106869 (2020).
- [32] Y. Núñez Fernández, M. K. Ritter, M. Jeannin, J.-W. Li, T. Kloss, T. Louvet, S. Terasaki, O. Parcollet, J. von Delft, H. Shinaoka, and X. Waintal, Learning tensor networks with tensor cross interpolation: New algorithms and libraries, *SciPost Physics* **18**, 104 (2025).
- [33] S. V. Dolgov and D. V. Savostyanov, Alternating minimal energy methods for linear systems in higher dimensions, *SIAM Journal on Scientific Computing* **36**, A2248 (2014).
- [34] Z. Meng, Y. Khoo, J. Li, and E. M. Stoudenmire, Recursive sketched interpolation: Efficient Hadamard products of tensor trains (2026), 2602.17974.
- [35] A. A. Michailidis, C. Fenton, and M. Kiffner, Element-wise multiplication of tensor trains, *SIAM Journal on Scientific Computing* **47**, B1158 (2025).
- [36] Z. Sun, J. Huang, C. Xiao, and C. Yang, HaTT: Hadamard avoiding TT recompression (2025), 2410.04385.
- [37] P. Cazeaux, M.-S. Dupuy, and R. F. Justiniano, Linear-scaling tensor train sketching (2026), 2603.11009.
- [38] See supplemental material at [url].
- [39] S. A. Goreinov and E. E. Tyrtyshnikov, Quasioptimality of skeleton approximation of a matrix in the chebyshev norm, *Doklady Mathematics* **83**, 374 (2011).
- [40] L. Devos, M. Van Damme, and J. Haegeman, MPSKit (2026).
- [41] L. Devos and J. Haegeman, TensorKit.jl: A julia package for large-scale tensor computations, with a hint of category theory (2025), 2508.10076.
- [42] I. V. Oseledets, Approximation of $2^d \times 2^d$ matrices using tensor decomposition, *SIAM Journal on Matrix Analysis and Applications* **31**, 2130 (2010).
- [43] M. Lindsey, Multiscale interpolative construction of quantized tensor trains (2023), 2311.12554.
- [44] J. Chen, E. Stoudenmire, and S. R. White, Quantum fourier transform has small entanglement, *PRX Quantum* **4**, 040318 (2023).
- [45] J. Chen and M. Lindsey, Direct interpolative construction of the discrete fourier transform as a matrix product operator, *Applied and Computational Harmonic Analysis* **81**, 101817 (2026).
- [46] V. A. Kazeev and B. N. Khoromskij, Low-rank explicit QTT representation of the laplace operator and its inverse, *SIAM Journal on Matrix Analysis and Applications* **33**, 742 (2012).
- [47] G. Grosso, M. K. Ritter, S. Rohshap, S. Badr, A. Kauch, M. Wallerberger, J. v. Delft, and H. Shinaoka, Adaptive patching for tensor train computations (2026), 2602.22372.
- [48] J. Tindall, M. Stoudenmire, and R. Levy, Compressing multivariate functions with tree tensor networks (2024), 2410.03572.
- [49] M. K. Ritter, Code repository for ‘Fast elementwise operations on tensor trains with alternating cross interpolation’, <https://doi.org/10.5281/zenodo.19208286>.
- [50] M. K. Ritter, AlternatingCrossInterpolation.jl (2026).
- [51] Tensor4all, tensor4all.org.

Supplemental Material:

Fast elementwise operations on tensor trains with alternating cross interpolation

Marc K. Ritter *

Center for Computational Quantum Physics, Flatiron Institute, 162 5th Avenue, New York, NY 10010, USA

S-1. COMPLEXITY ANALYSIS

The three steps of each local update scale as follows.

1. Contracting the frame matrices of size $\chi' \times \chi$ with the input tensors X_ℓ^n and $X_{\ell+1}^n$ of size $\chi \times d \times \chi$ costs $\mathcal{O}(d\chi^2\chi' + d^2\chi\chi'^2)$ for each input x^n (Eq. (10)).
2. The function evaluation $f(\Pi_\ell^1, \dots, \Pi_\ell^N)$ costs $\mathcal{O}(d^2\chi'^2)$ (Eq. (11)).
3. Finally, factorizing Π_ℓ to obtain index sets can be done in $\mathcal{O}(d\chi'^3)$ (Eq. (11)).

Each local update therefore scales as $\mathcal{O}(Nd\chi^2\chi' + Nd^2\chi\chi'^2 + d\chi'^3)$. Since the local update is done $\mathcal{L}N_{\text{sweep}}$ times, the total runtime cost is $t \in \mathcal{O}(\mathcal{L}N_{\text{sweep}}[Nd\chi^2\chi' + d^2(N\chi + \chi')\chi'^2])$. We can distinguish three common cases by the dependence of χ' on χ :

1. $\chi' = \text{const.} \Rightarrow t \in \mathcal{O}(\mathcal{L}N_{\text{sweep}}N[d\chi^2 + d^2\chi])$.
In this case, the output bond dimension is independent of χ . The contraction of the input tensors X_ℓ^n to form frame matrices dominates the runtime (Eq. (8)).
2. $\chi' \in \mathcal{O}(\chi) \Rightarrow t \in \mathcal{O}(\mathcal{L}N_{\text{sweep}}Nd^2\chi^3)$.
The output and input are of comparable complexity, which is the case considered in the main text. The runtime is dominated by contracting frame matrices onto X_ℓ^n to form the tensor Π_ℓ^n in each local update (Eq. (10)).
3. $\chi' \in \mathcal{O}(\chi^2) \Rightarrow t \in \mathcal{O}(\mathcal{L}N_{\text{sweep}}d^2[N\chi^5 + \chi^6])$.
The output has maximum bond dimension. The runtime is dominated by the cost of factorizing the tensor Π_ℓ (Eq. (11)).

In the common case where the elementwise operation to be computed is a Hadamard product, the most widely used alternative to ACI is a contraction with a diagonal tensor train, as described in e.g. Refs. 12 and 13. The complexity of that algorithm is dominated by the cost of tensor train contraction (MPO-MPS contraction), for which algorithms with scaling $\mathcal{O}(\mathcal{L}d^2\chi^4)$ are known [21–24]. ACI has better scaling compared to MPO-MPS contraction when $\chi' \in \mathcal{O}(\chi^{4/3})$.

S-2. ALGORITHMS IN PSEUDOCODE

The main alternating cross interpolation (ACI) algorithm is presented in Alg. 1, with helper functions defined in Algs. 2, 3, 4, and 5. For brevity, we use the following conventions in the pseudocode:

- Index names: σ_ℓ are always local (site) indices. i and j are reserved for multi-indices that are part of some index sets \mathcal{I} and \mathcal{J} . All other indices without special properties are given Greek letters α, β, γ .
- Submatrices: To take submatrices and re-order rows and columns, we put index sets \mathcal{I} and \mathcal{J} in the indices of a matrix. For example, $B = A_{\mathcal{I}, \mathcal{J}}$ means that B is the truncation of A to the rows in \mathcal{I} and columns in \mathcal{J} .
- Index ranges: We use the notation $m : n := (m, m + 1, \dots, n - 1, n)$ to express index ranges.
- Indexed assignment: When indices appear on both sides of an assignment, this assignment is understood as assigning all elements. For example, $A_{\alpha,1} \leftarrow B_{\alpha,1}$ means

```

for  $\alpha \in \{1, \dots, \text{nrows}(A)\}$  do
   $A_{\alpha,1} \leftarrow B_{\alpha,1}$ 

```

- Einstein summation: Whenever an index appears on two or more elements that are being multiplied, that multiplication is to be understood as a contraction over that index. For example, $C_{\alpha\beta} \leftarrow A_{\alpha\gamma} B_{\gamma\beta}$ is equivalent to the matrix product $C \leftarrow AB$.

An implementation of ACI in the Julia programming language can be found online [50] as part of the tensor4all open-source libraries [51].

Algorithm1 The alternating cross interpolation (ACI) algorithm.

ACI	
Input	f elementwise function X^1, \dots, X^N input tensor trains Y^{init} initial guess for Y ; if nothing is known, initialize randomly. τ absolute error tolerance $\hat{\chi}$ maximum bond dimension $maxiter$ number of iterations (sweeps)
Output	Y a tensor train approximating $Y_{\sigma} \approx f(X_{\sigma}^1, \dots, X_{\sigma}^N)$
<pre> 1: for $n \leftarrow 1, \dots, N$ do 2: $L_0^n \leftarrow [1]$ ▷ Initialize first left frame matrix as 1×1 matrix. 3: $R_{\mathcal{L}+1}^n \leftarrow [1]$ ▷ Analogous for last right frame matrix. 4: for $\ell \leftarrow \mathcal{L}, \mathcal{L} - 1, \dots, 2$ do ▷ Bring initial guess into CI-canonical form as described in Ref. 32. (Eq. (5)) 5: $M_{\alpha, \sigma_{\ell} j} \leftarrow [Y_{\ell}^{\text{init}}]_{\alpha, j}^{\sigma_{\ell}}$ ▷ Reshape site tensor to matrix. 6: $M', Y_{\ell}, -, \mathcal{J}_{\ell} \leftarrow \text{CROSSINTERPOLATE}(M, \tau, \hat{\chi})$ ▷ The row indices are not meaningful here, and are discarded. 7: $[Y_{\ell-1}]_{\alpha\beta}^{\sigma} \leftarrow [Y_{\ell-1}]_{\alpha\gamma}^{\sigma} M'_{\gamma\beta}$ ▷ Multiply left factor M' to the left. 8: for $n \leftarrow 1, \dots, N$ do ▷ Initialize right frames iteratively. (Alg. 5, Eq. (8)) 9: $R_{\ell}^n \leftarrow \text{RIGHTFRAME}(X_{\ell}^n, R_{\ell+1}^n, \mathcal{J}_{\ell})$ 10: for $iteration \leftarrow 1, \dots, maxiter$ do ▷ Main loop. 11: for $\ell \leftarrow 1, 2, \dots, \mathcal{L} - 1$ do ▷ Left-to-right sweep. 12: $[\Pi^n]_{\sigma_{\ell}, \sigma_{\ell+1}} \leftarrow L_{\ell-1}^n [X_{\ell}^n]^{\sigma_{\ell}} [X_{\ell+1}^n]^{\sigma_{\ell+1}} R_{\ell+2}^n$ ▷ Assemble Π^n in interpolative basis. (Eq. (10)) 13: $\Pi_{\alpha, \beta}^{\sigma_{\ell}, \sigma_{\ell+1}} \leftarrow f([\Pi^1]_{\alpha, \beta}^{\sigma_{\ell}, \sigma_{\ell+1}}, \dots, [\Pi^N]_{\alpha, \beta}^{\sigma_{\ell}, \sigma_{\ell+1}})$ ▷ Apply elementwise operation f. (Eq. (11)) 14: $Y_{\ell}, Y_{\ell+1}, \mathcal{I}_{\ell}, \mathcal{J}_{\ell+1}, \epsilon_{\ell} \leftarrow \text{LOCALUPDATE}(\Pi, \tau, \hat{\chi}, \text{right})$ ▷ Update bond $(\ell, \ell + 1)$. (Alg. 4, Eq. (11)) 15: $L_{\ell}^n \leftarrow \text{LEFTFRAME}(X_{\ell}^n, L_{\ell-1}^n, \mathcal{I}_{\ell})$ ▷ Update frame matrix. (Alg. 5, Eq. (8)) 16: for $\ell \leftarrow \mathcal{L} - 1, \dots, 2, 1$ do ▷ Right-to-left sweep. 17: $[\Pi^n]_{\sigma_{\ell}, \sigma_{\ell+1}} \leftarrow L_{\ell-1}^n [X_{\ell}^n]^{\sigma_{\ell}} [X_{\ell+1}^n]^{\sigma_{\ell+1}} R_{\ell+2}^n$ ▷ Assemble Π^n in interpolative basis. (Eq. (10)) 18: $\Pi_{\alpha, \beta}^{\sigma_{\ell}, \sigma_{\ell+1}} \leftarrow f([\Pi^1]_{\alpha, \beta}^{\sigma_{\ell}, \sigma_{\ell+1}}, \dots, [\Pi^N]_{\alpha, \beta}^{\sigma_{\ell}, \sigma_{\ell+1}})$ ▷ Apply elementwise operation f. (Eq. (11)) 19: $Y_{\ell}, Y_{\ell+1}, \mathcal{I}_{\ell}, \mathcal{J}_{\ell+1}, \epsilon_{\ell} \leftarrow \text{LOCALUPDATE}(\Pi, \tau, \hat{\chi}, \text{left})$ ▷ Update bond $(\ell, \ell + 1)$. (Alg. 4, Eq. (11)) 20: $R_{\ell+1}^n \leftarrow \text{RIGHTFRAME}(X_{\ell+1}^n, R_{\ell+2}^n, \mathcal{J}_{\ell+1})$ ▷ Update frame matrix. (Alg. 5, Eq. (8)) 21: if χ_{ℓ} have not increased & $\max_{\ell} \epsilon_{\ell} \leq \tau$ then 22: break </pre>	

Algorithm2 In-place LDU factorization of a matrix M using the prrLU algorithm of Ref. [32].

LDU

Input M a $m \times n$ matrix to be factorized
 τ truncation tolerance
 $\hat{\chi}$ maximum bond dimension

Output L a lower triangular matrix,
 D a diagonal matrix, and
 U an upper triangular matrix, such that $LDU \approx M$.
 \mathcal{I}, \mathcal{J} row and column index set
 ϵ error estimate

1: $\mathcal{I} \leftarrow (1, 2, \dots, m)$
2: $\mathcal{J} \leftarrow (1, 2, \dots, n)$
3: $\chi \leftarrow 1$
4: **repeat**
5: $i, j \leftarrow \operatorname{argmax}_{\alpha \geq \chi, \beta \geq \chi} |M_{\alpha, \beta}|$ \triangleright Find next pivot using a greedy version of the maxvol principle.
6: $\operatorname{swap}(M_{i, 1:n}, M_{\chi, 1:n})$ \triangleright Swap the next pivot to position (χ, χ) in M .
7: $\operatorname{swap}(M_{1:m, j}, M_{1:m, \chi})$
8: $\operatorname{swap}(\mathcal{I}_i, \mathcal{I}_\chi)$ \triangleright Update \mathcal{I} and \mathcal{J} accordingly.
9: $\operatorname{swap}(\mathcal{J}_i, \mathcal{J}_\chi)$
10: $M_{\chi+1:m, \chi+1:n} \leftarrow M_{\chi+1:m, \chi+1:n} - M_{\chi:m, \chi} [M_{\chi, \chi}]^{-1} M_{\chi, \chi:n}$ \triangleright Schur complement (Gaussian elimination step).
11: $\epsilon \leftarrow |M_{\chi, \chi}|$ \triangleright Error estimate.
12: **until** $\epsilon \leq \tau$ or $\chi = \hat{\chi}$
13: $L \leftarrow \operatorname{lowertriangle}(M_{1:m, 1:\chi})$ $\triangleright L, D,$ and U are now in different parts of M .
14: $D \leftarrow \operatorname{diagonal}(M_{1:\chi, 1:\chi})$
15: $U \leftarrow \operatorname{uppertriangle}(M_{1:\chi, 1:n})$
16: $\mathcal{I}, \mathcal{J} \leftarrow \mathcal{I}_{1:\chi}, \mathcal{J}_{1:\chi}$

Algorithm3 Cross interpolation (CI) of a matrix M in a stable manner using LDU factorization. Adapted from Ref. [32].

CROSSINTERPOLATE

Input M a $m \times n$ matrix to be factorized
 τ truncation tolerance
 $\hat{\chi}$ maximum bond dimension
 $leftorright$ whether to multiply the factor P^{-1} to the left or the right factor

Output A left factor, and
 B right factor, such that $AB \approx M$.
 $\mathcal{I}_{1:\chi}, \mathcal{J}_{1:\chi}$ row and column index set
 ϵ error estimate

1: $L, D, U, \mathcal{I}, \mathcal{J}, \epsilon \leftarrow \operatorname{LDU}(M, \tau, \hat{\chi})$ \triangleright (Alg. 2)
2: **if** $leftorright = \text{left}$ **then** \triangleright Left-orthogonal case.
3: $A \leftarrow L [L_{\mathcal{I}, 1:n}]^{-1}$
4: $B \leftarrow L_{\mathcal{I}, 1:n} D U$
5: **else** \triangleright Right-orthogonal case.
6: $A \leftarrow L D U_{1:m, \mathcal{J}}$
7: $B \leftarrow [U_{1:m, \mathcal{J}}]^{-1} U$

Algorithm4 Computes the factors $Y_\ell, Y_{\ell+1}$ for the local update in AC (see Eq. (11)).

LOCALUPDATE

Input Π a two-site tensor (see Eq. (10))
 τ truncation tolerance
 $\hat{\chi}$ maximum bond dimension
leftorright whether to multiply the factor P^{-1} to the left or the right factor (see Eq. (4))

Output Y, Y' left and right factor, such that $\Pi_{\alpha\beta}^{\sigma\sigma'} \approx Y_{\alpha\gamma}^\sigma Y_{\gamma\beta}'^{\sigma'}$
 $\mathcal{I}_{1:\chi}, \mathcal{J}_{1:\chi}$ row and column index set
 ϵ error estimate

1: $M_{\alpha\otimes\sigma,\sigma'\otimes\beta} \leftarrow \Pi_{\alpha\beta}^{\sigma,\sigma'}$ ▷ Reshape Π to a matrix.
2: $A, B, \mathcal{I}, \mathcal{J}, \epsilon \leftarrow \text{CROSSINTERPOLATE}(M, \tau, \hat{\chi}, \textit{leftorright})$ ▷ Factorize matricized Π . (Alg. 3)
3: $Y_{\alpha\beta}^\sigma \leftarrow A_{\alpha\otimes\sigma,\beta}$ ▷ Reshape the matrix factors to tensor form.
4: $Y_{\alpha\beta}'^{\sigma'} \leftarrow B_{\alpha,\sigma'\otimes\beta}$

Algorithm5 Iterative construction of left and right frame matrices (Eq. (8)).

LEFTFRAME

Input X tensor for site ℓ (size $\chi_L \times d \times \chi_R$)
 L left frame for sites $1, \dots, \ell - 1$
 \mathcal{I} index set for truncation of output frame

Output L' left frame for sites $1, \dots, \ell$

1: $L'_{i\sigma,\beta} \leftarrow L_{i,\gamma} X_{\gamma,\beta}^\sigma$ ▷ $i\sigma = (i_1, \dots, i_{\ell-1}, \sigma)$
2: $L' \leftarrow L'_{\mathcal{I},1:\chi_R}$ ▷ Truncate rows according to \mathcal{I} .

RIGHTFRAME

Input X tensor for site ℓ (size $\chi_L \times d \times \chi_R$)
 R right frame for sites $\ell + 1, \dots, \mathcal{L}$
 \mathcal{J} index set for truncation of output frame

Output L' left frame for sites $1, \dots, \ell$

1: $R'_{\alpha,\sigma j} \leftarrow X_{\alpha,\gamma}^\sigma R_{\gamma,j}$ ▷ $\sigma j = (\sigma, j_{\ell+1}, \dots, j_{\mathcal{L}})$
2: $R' \leftarrow R'_{1:\chi_L,\mathcal{J}}$ ▷ Truncate columns according to \mathcal{J} .
